

## A Self-Locking Molecule Operative with a Photoresponsive Key

Takahiro Muraoka,<sup>†</sup> Kazushi Kinbara,<sup>\*,‡</sup> and Takuzo Aida<sup>\*</sup>

Contribution from Department of Chemistry and Biotechnology, School of Engineering, and Center for NanoBio Integration, The University of Tokyo, 7-3-1 Hongo, Bunkyo-ku, Tokyo 113-8656, Japan, and PRESTO, Japan Science Technology Agency (JST), 4-1-8 Honcho, Kawaguchi, Saitama 332-0012, Japan

Received May 9, 2006; E-mail: kinbara@macro.t.u-tokyo.ac.jp; aida@macro.t.u-tokyo.ac.jp

**Abstract:** Rotary host **1**, composed of a ferrocene unit as a rotary module, is conformationally locked internally in apolar solvents such as benzene by a double intramolecular Zn–N coordination between the zinc porphyrin and aniline units, attached to each cyclopentadienyl (Cp) ring. Upon addition of the *cis* form of 1,2-bispyridylethylene (*cis*-**2**) to (+)-**1** ( $[cis-2]/[(+)-1] = 5.0$ ), an enantiomer of **1**, the intramolecular Zn–N coordination bonds in (+)-**1** are readily cleaved to form an externally locked, cyclodimeric one-to-one complex (+)-**1**⊃*cis*-**2**, accompanying a rotation of the ferrocene module, as visualized by CD spectroscopy. In contrast, use of *trans*-**2**, in place of *cis*-**2**, under otherwise identical conditions to the above, did not result in releasing the internal double lock of (+)-**1**. Such a large difference between the isomers of **2** in the affinity toward host **1**, along with their capabilities of photochemical interconversion, allowed for the demonstration of a reversible self-locking operation of **1**. Namely, the externally locked state of **1**, as in the form of **1**⊃*cis*-**2**, spontaneously retrieves the internally locked state, after the release of **2** from **1** upon *cis*-to-*trans* photochemical isomerization of ligating **2**, while the backward photochemical isomerization of **2** in the presence of **1** results in switching of **1** to its externally locked state.

### Introduction

Self-locking systems are useful for fail-safe operations and utilized for a variety of equipments in our daily life. An essential feature of self-locking systems is that they are normally locked and kept dormant, while they can be unlocked with proper keys whenever necessary. Furthermore, when the keys are released, self-locking systems automatically retrieve the locked states. Such self-locking mechanisms are also seen in biological systems, especially in signal transduction pathways.<sup>1</sup> For example, Ca<sup>2+</sup>/calmodulin-dependent protein kinase II (CaM-kinase II) is the representative of self-locking enzymes.<sup>2</sup> In its resting state, the active site is hybridized with an autoinhibitory segment and sterically protected from the access of substrates. On the other hand, once cofactor calmodulin binds Ca<sup>2+</sup>, it

undergoes a conformational change and wraps around the autoinhibitory segment to allow its dissociation from the active site. Hence, the enzyme is activated to start phosphorylation. However, when Ca<sup>2+</sup> is dissociated from calmodulin, the autoinhibitory segment is liberated from calmodulin and allowed to reassemble with the active site of the enzyme. Consequently, CaM-kinase II automatically returns to its resting state. Thus, in this sequential event, calmodulin is the key to switch on and off the enzymatic activity of self-locking CaM-kinase II, while Ca<sup>2+</sup> serves to activate the “calmodulin” key to change the priority of the two competing interactions involving the autoinhibitory segment.

In the present paper, we report a novel artificial self-locking system, designed by combining rotary host **1** (Figure 1) carrying internal locking units with photochromic 1,2-bispyridylethylene **2** as an external key.<sup>3</sup> The self-locking operation of **1** was demonstrated by a photochemical priority change of competing intra- and intermolecular interactions (Scheme 1).<sup>4</sup>

<sup>†</sup> The University of Tokyo.

<sup>‡</sup> PRESTO, JST.

- (1) (a) *Introduction to Cellular Signal Transduction*; Ari, S., Ed.; Birkhauser: New York, 1999. (b) *Biochemistry of Signal Transduction and Regulation*; Krauss, G.; John Wiley & Sons: New York, 1999. (c) Schlessinger, J. *Cell* **2000**, *103*, 211–225. (d) Pawson, T.; Nash, P. *Genes Dev.* **2000**, *14*, 1027–1047. (e) Hlsken, J.; Behrens, J. *J. Cell Sci.* **2000**, *113*, 3545–3546. (f) Leever, S. J.; Vanhaesebroeck, B.; Waterfield, M. D. *Curr. Opin. Cell Biol.* **1999**, *11*, 219–225. (g) Chan, Y. M.; Jan, Y. N. *Cell* **1998**, *94*, 423–426. (h) Ghosh, S.; May, M.; Kopp, E. *Annu. Rev. Immunol.* **1998**, *16*, 225–260. (i) Neel, B. G.; Tonks, N. K. *Curr. Opin. Cell Biol.* **1997**, *9*, 192–204. (j) Pitcher, J. A.; Freedman, N. J.; Lefkowitz, R. J. *Annu. Rev. Biochem.* **1998**, *67*, 653–692. (k) Pawson, T.; Scott, J. D. *Science* **1997**, *278*, 2075–2080. (l) Bourne, H. R. *Curr. Opin. Cell Biol.* **1997**, *9*, 134–142. (m) Darnell, J. E., Jr.; Kerr, I. M.; Stark, G. R. *Science* **1994**, *264*, 1415–1421. (n) Nishizuka, Y. *Science* **1992**, *258*, 607–614.
- (2) (a) Schulman, H. *Curr. Opin. Cell Biol.* **1993**, *5*, 247–253. (b) Hanson, P. I.; Schulman, H. *Annu. Rev. Biochem.* **1992**, *61*, 559–601. (c) Morris, R. G. M.; Kennedy, M. B. *Curr. Biol.* **1992**, *2*, 511–514.

- (3) Selected reviews of photochromic compounds: (a) Irie, M. *Chem. Rev.* **2000**, *100*, 1685–1716. (b) Yokoyama, Y. *Chem. Rev.* **2000**, *100*, 1717–1739. (c) Berkovic, G.; Krongauz, V.; Weiss, V. *Chem. Rev.* **2000**, *100*, 1741–1753. (d) Feringa, B. L.; van Delden, R. A.; Koumura, N.; Geertsema, E. M. *Chem. Rev.* **2000**, *100*, 1789–1816.
- (4) Examples of photoswitchable host–guest systems: (a) *Molecular Switches*; Feringa, B. L., Ed.; Wiley-VCH: Weinheim, 2001. (b) Balzani, V.; Credi, A.; Marchioni, F.; Stoddart, J. F. *Chem. Commun.* **2001**, 1860–1861. (c) Takeshita, M.; Uchida, K.; Irie, M. *Chem. Commun.* **1996**, 1807–1808. (d) Willner, I.; Marx, S.; Eichen, Y. *Angew. Chem., Int. Ed.* **1992**, *31*, 1243–1244. (e) Shinkai, S.; Nakaji, T.; Ogawa, T.; Shigematsu, K.; Manabe, O. *J. Am. Chem. Soc.* **1981**, *103*, 111–115.

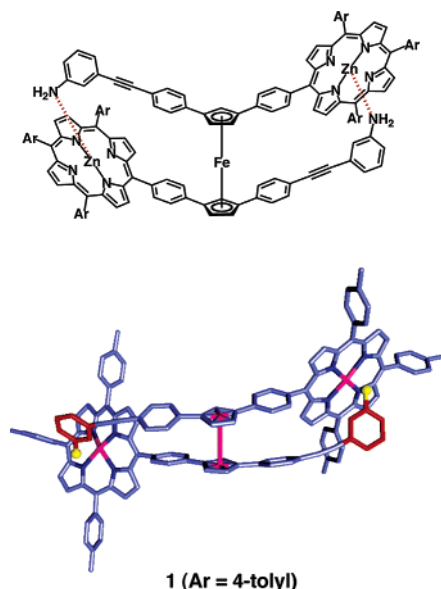


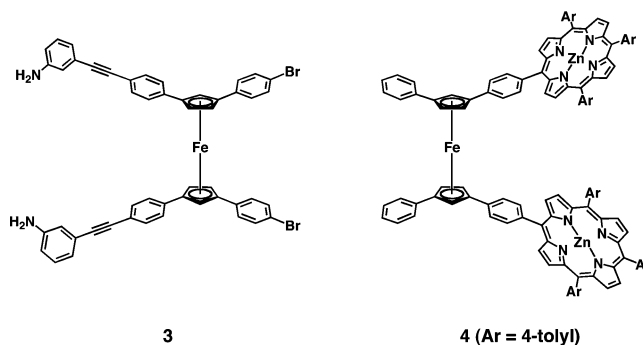
**Figure 1.** Molecular model of internally double-locked **1**. Red and yellow parts denote aromatic and amino groups of the aniline units, respectively. Pink parts represent zinc atoms coordinating with the aniline amino groups. The iron atom of the ferrocene module is represented in purple. Hydrogen atoms are omitted for clarity. The structure was optimized by a molecular mechanics calculation with an MMFF force field using Spartan'02.

## Results and Discussion

Host **1** is composed of a ferrocene unit as a rotary module,<sup>5</sup> which bears zinc porphyrin and aniline units at each cyclopentadienyl (Cp) ring. The rotary motion of **1** allows the aniline groups to come closer to the zinc porphyrin units, forming two Zn–N coordination bonds simultaneously.<sup>6</sup> Although the interaction between zinc porphyrins and aniline is rather weak, such a double intramolecular Zn–N coordination is strong enough to lock the rotary motion of **1** (internal double lock) (Figure 1). Thus, host **1** is self-locked in appropriate apolar solvents such as benzene. On the other hand, compound **2** bears two pyridine units, capable of coordinating to the zinc porphyrin units in **1**, in competition with the internal aniline groups. This compound is photochromic, where UV irradiation allows for its trans-to-cis isomerization,<sup>7</sup> while visible light irradiation in the presence of triplet sensitizers such as zinc porphyrins allows for the backward isomerization.<sup>8</sup> We found that rotary host **1** is kept self-locked conformationally when mixed with, e.g., 5 equiv of compound **2** adopting a trans configuration (*trans*-**2**), since **1** hardly interacts with *trans*-**2** under the conditions employed (Scheme 1, top right). However, when **2** is photochemically isomerized into its cis form, **1** turns to accommodate resultant *cis*-**2** at its binding site, to form stable cyclodimeric **1**⊃*cis*-**2** having two zinc–pyridyl coordination bonds (Scheme 1, left). Namely, the internal double lock is released, and **1** is transformed into an externally locked state. On the other hand, when

*cis*-**2** in **1**⊃*cis*-**2** is isomerized into its trans form, resultant *trans*-**2** detaches from rotary host **1**, thereby disabling the external locking. Consequently, **1** spontaneously retrieves, via a rotary motion, the internally double-locked state. Thus, compound **2** is regarded as a photoresponsive key for executing the self-locking operation of **1**. Rotary host **1** has a planar chirality at the ferrocene module, and use of the enantiomers of **1** could enable chiroptical visualization of its conformational motions in response to the photochemical isomerization of **2**.<sup>9</sup>

**Synthesis and Conformational Aspects of Host (+)-1.** Dibromoferrocene derivative **3** having two aniline units,<sup>9</sup> in a racemic form, was subjected to preparative chiral HPLC on a column Chiralpak IA. One of the enantiomers of **3**, eluted slower, was allowed to react with a zinc porphyrin boronate (see Experimental Section for details), and resulting compound **1** was unambiguously characterized by means of <sup>1</sup>H NMR spectroscopy and MALDI-TOF-MS spectrometry, along with electronic absorption, circular dichroism (CD), and infrared (IR) spectroscopies. Host **1** displayed absorption bands at 280–390 nm in benzene due to the ferrocene module, along with intense visible absorption bands at 433.5 (Soret band), 563.0, and 605.0 nm (Q-bands) due to the zinc porphyrin units. Host **1** is enantiomerically denoted as (+)-**1**, as it showed intense positive CD bands at 353.4 and 436.8 nm, along with a weak negative CD band at 303.4 nm (see Supporting Information, Figure S1).



Rotary host (+)-**1** in benzene displayed absorptions in the Soret and Q-band regions at 433.5, 563.0, and 605.0 nm, which are obviously red shifted from those of reference compound **4** without aniline units (424.5, 522.0, and 591.0 nm; see Supporting Information, Figure S2). This spectral profile is attributable to an intramolecular coordination between the zinc porphyrin and aniline units.<sup>6</sup> Upon incremental increase of the concentration from 10<sup>−7</sup> to 10<sup>−4</sup> M, neither the electronic absorption nor the CD bands of (+)-**1** exhibited any shifts, but they were monotonically enhanced, following the Lambert–Beer's law (Figure 2). In the <sup>1</sup>H NMR spectrum of (+)-**1** in benzene-*d*<sub>6</sub>, a characteristic signal due to aniline NH<sub>2</sub> appeared at δ −2.89 ppm,<sup>10</sup> indicating that the aniline groups coordinate to the zinc porphyrin units and are magnetically shielded (Figure 3).<sup>6</sup> Considering the molecular structure, these spectral profiles clearly indicate that **1** is in a self-locked state by adopting a head-to-tail geometry with the two intramolecular Zn–N coordination bonds (internal double lock; Figure 1).

**Complexation Behaviors of (+)-1 with *trans*- and *cis*-2.** According to CPK model studies, *trans*-**2** adopts an extended

(5) Gardner, A. B.; Howard, J.; Waddington, T. C.; Richardson, R. M.; Tomkinson, J. *Chem. Phys.* **1981**, 57, 453–460.

(6) (a) Borovkov, V. V.; Hembury, G. A.; Inoue, Y. *Acc. Chem. Res.* **2004**, 37, 449–459. (b) Huang, X.; Fujioka, N.; Pescitelli, G.; Koehn, F. E.; Williamson, R. T.; Nakanishi, K.; Berova, N. *J. Am. Chem. Soc.* **2002**, 124, 10320–10335.

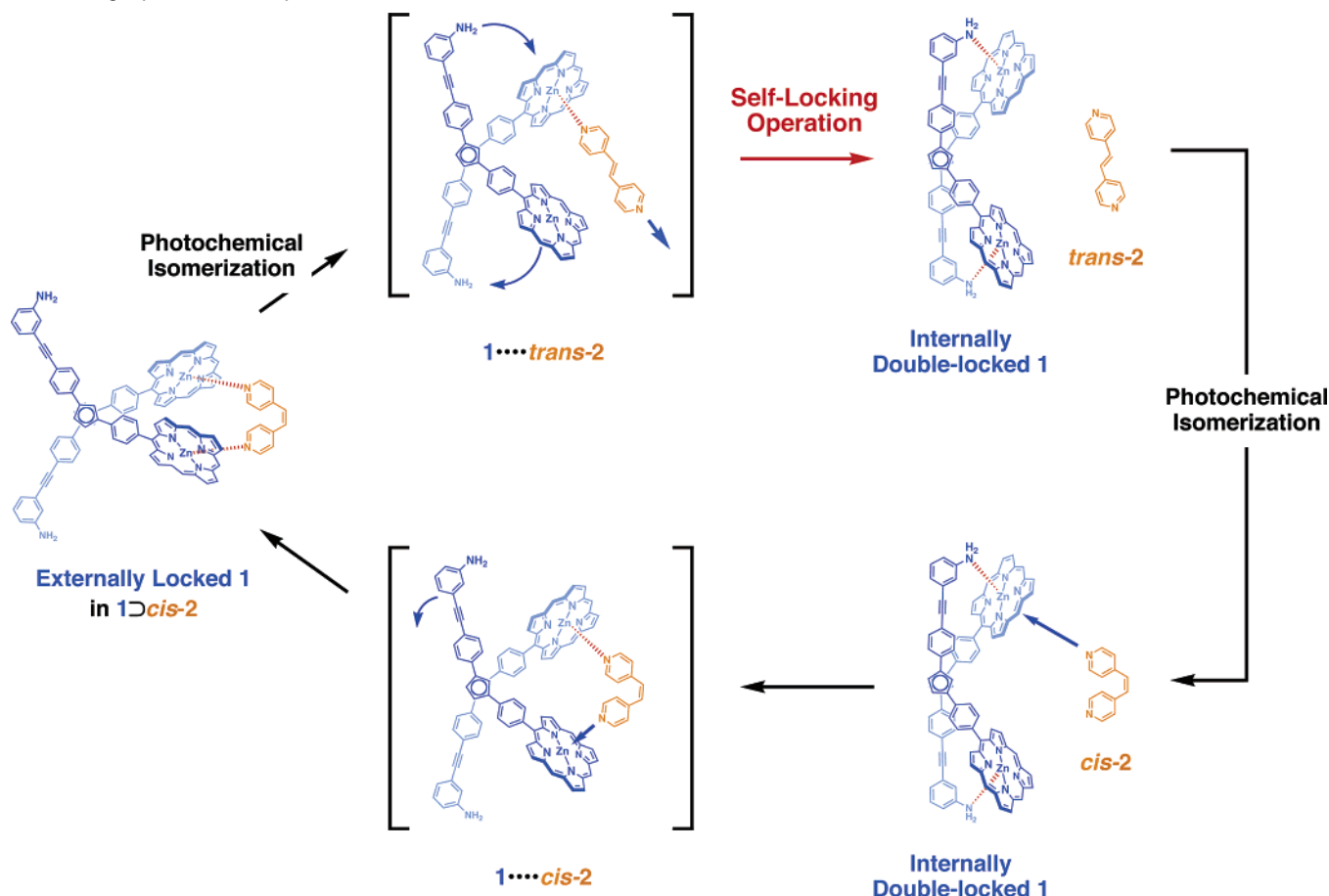
(7) Itokazu, M. K.; Polo, A. S.; Araújo de Faria, D. L.; Bignozzi, C. A.; Murakami Iha, N. Y. *Inorg. Chim. Acta* **2001**, 313, 149–155.

(8) (a) Iseki, Y.; Watanabe, E.; Mori, A.; Inoue, S. *J. Am. Chem. Soc.* **1993**, 115, 7313–7317. (b) Whitten, D. G.; Wildes, P. D.; DeRosier, C. A. *J. Am. Chem. Soc.* **1972**, 94, 7811–7823. (c) Whitten, D. G.; McCall, M. T. *J. Am. Chem. Soc.* **1969**, 91, 5097–5103.

(9) (a) Muraoka, T.; Kinbara, K.; Aida, T. *Nature* **2006**, 440, 512–515. (b) Muraoka, T.; Kinbara, K.; Kobayashi, Y.; Aida, T. *J. Am. Chem. Soc.* **2003**, 125, 5612–5613.

(10) This signal was not observed when the solvent contains D<sub>2</sub>O.

**Scheme 1.** Molecular Structures of Internally Double-Locked **1** and Externally Locked **1**⊃*cis*-**2**, and Schematic Representation of the Self-locking Operation in Response to Photochemical Isomerization of **2**<sup>a</sup>



<sup>a</sup> Ar groups are omitted for clarity.

geometry, while *cis*-**2** adopts an angular geometry. Interestingly, we found that these two isomeric forms show quite different affinities toward host **1**, where *cis*-**2** is much favored over *trans*-**2**. Upon titration with *cis*-**2** at 20 °C in benzene, electronic absorption spectroscopy of (+)-**1** ( $2.4 \times 10^{-6}$  M) displayed a blue shift in the Soret absorption band from 433.5 to 428.0 nm with a clear isosbestic point at 430.0 nm. This spectral change appeared to take place monotonically and then saturated at a [*cis*-**2**]/[(+)-**1**] mole ratio of 7.0 (see Supporting Information,

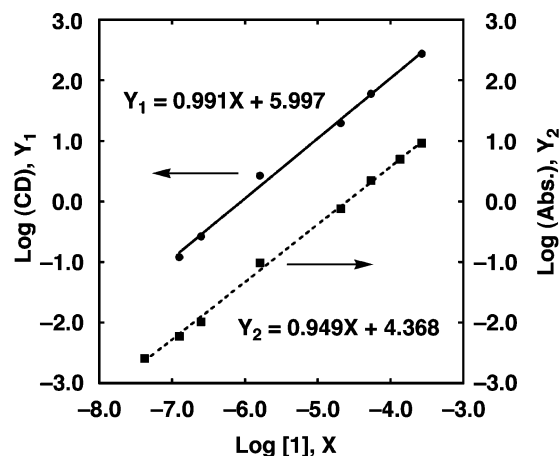


**Figure 2.** Concentration dependencies of the circular dichroism (CD) intensity (●, solid line,  $Y_1$ ) and absorbance (■, broken line,  $Y_2$ ) of (+)-**1** at 352.0 nm in benzene at 20 °C.

Figure S3). The Job's plot, upon mixing (+)-**1** with *cis*-**2** in benzene, showed an absorption maximum at a [*cis*-**2**]/[(+)-**1**] mole ratio of unity (Figure 4a). Considering the monotonic spectral change in the titration experiment, we conclude that (+)-**1** and *cis*-**2** form a cyclodimeric one-to-one complex (+)-**1**⊃*cis*-**2** with only a negligibly small spectral contribution, if any, of its acyclic intermediate. From these results, the association constant  $K_{\text{assoc}}$  of (+)-**1** with *cis*-**2** was evaluated as  $7.5 \times 10^5$  M<sup>-1</sup> (see Supporting Information, Figure S4a), which is roughly 2 orders of magnitude greater than that of (+)-**1** with pyridine (see Supporting Information, Figures S4b and S5). Such a large  $K_{\text{assoc}}$  value is obviously due to the two-point complexation between (+)-**1** and *cis*-**2** (Figure 4, top). Namely, the

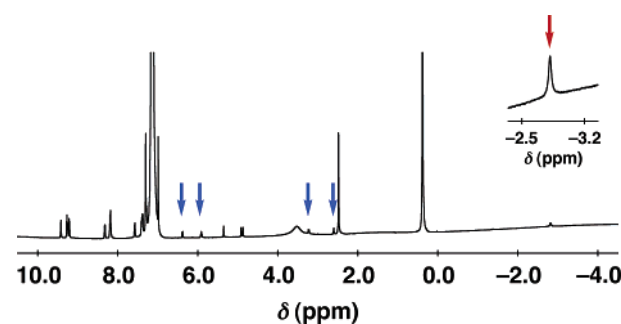


**Figure 3.** <sup>1</sup>H NMR spectrum of (+)-**1** in C<sub>6</sub>D<sub>6</sub> at 20 °C. Red and blue arrows represent the signals due to the amino and aromatic protons of the aniline groups, respectively. Inset: An enlarged spectrum at the amino proton region.

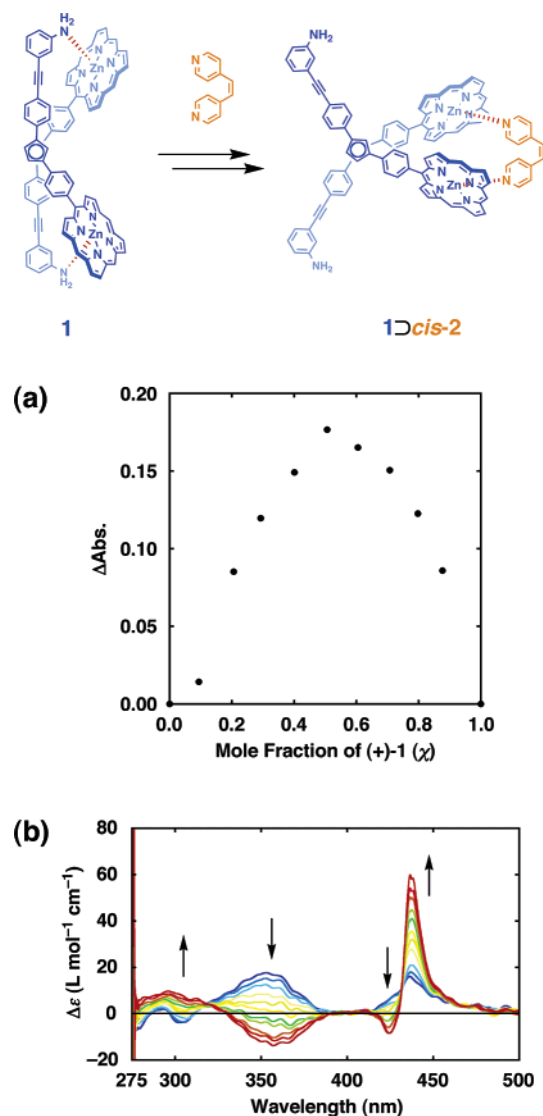


**Figure 4.** (a) Job's plot upon mixing (+)-**1** with *cis*-**2** in benzene at 20 °C. (b) Circular dichroism (CD) spectral change of (+)-**1** in benzene ( $2.4 \times 10^{-6}$  M) at 20 °C upon titration with *cis*-**2** ( $[cis-2]/[(+)-1] = 0.0, 0.12, 0.23, 0.46, 0.70, 0.93, 1.4, 1.9, 2.8, 3.7,$  and  $7.0$ ). Arrows indicate the directions of spectral changes.

internally double-locked state of **1** can be unlocked by the coordination with *cis*-**2**. We also found that the absorption spectral change in the titration experiment (Figure S3) is accompanied by a large, monotonic CD spectral change at the absorption bands of the zinc porphyrin and ferrocene units, exhibiting isosbestic points at 318.6 and 431.6 nm (Figure 4b). The CD spectral change at the absorption band of the ferrocene unit is indicative of its rotary motion accompanied by the coordination with *cis*-**2** (Figure 4, top). On the other hand, the appearance of the marked split Cotton effect at the Soret absorption band of (+)-**1**·*cis*-**2** (415–455 nm) indicates that the two zinc porphyrin units in (+)-**1** are forced, by ligation with *cis*-**2**, to come closer to one another and undergo exciton coupling.<sup>6</sup>

In sharp contrast, when *trans*-**2** was used in place of *cis*-**2**, (+)-**1** displayed only a subtle absorption spectral change upon addition of even 200 equiv of *trans*-**2** with respect to (+)-**1**. Nevertheless, at a closer look, the spectral change took place little by little until the guest/host ratio reached 3000 (see

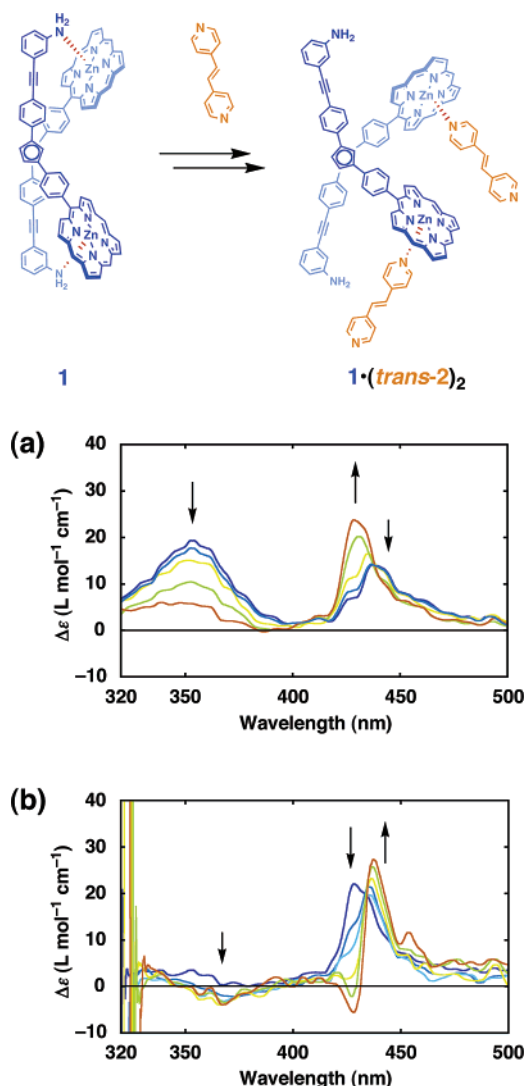


**Figure 5.** Circular dichroism (CD) spectral changes of (+)-**1** in benzene ( $2.5 \times 10^{-6}$  M) at 20 °C upon titration with *trans*-**2** ( $[trans-2]/[(+)-1] =$  (a)  $0, 5, 10, 40, 100$ , (b)  $200, 400, 600, 1000, 1400,$  and  $3000$ ). Arrows indicate the directions of spectral changes.

Supporting Information, Figure S6). Although this absorption spectral change appeared to be monotonic, the accompanying CD spectral change (Figure 5), though moderate, displayed a rather complicated dependence on the guest/host ratio and essentially different from that observed with *cis*-**2** as the guest (Figure 4b). With  $[trans-2]/[(+)-1]$  up to 100, the CD spectrum changed most explicitly at the absorption bands of the zinc porphyrin and ferrocene units, exhibiting isosbestic points at 402.6 and 438.8 nm (Figure 5a). While such a CD spectral change once appeared to subside with  $[trans-2]/[(+)-1]$  in a range from 100 to 200, further incremental increase of the guest/host ratio again resulted in a clear spectral change (isosbestic point = 433.6 nm) but only at the zinc porphyrin absorption (Figure 5b). When the guest/host ratio was greater than 3000, the CD spectrum of (+)-**1** no longer changed. Such a complicated CD spectral change likely originates from the extended geometry of *trans*-**2** capable of forming, upon interaction with **1**, macrocyclic and linear polymeric structures, along with 1:1 and 2:1 acyclic guest/host complexes. For the monotonic change in Figure S6, these species are likely indistinguishable from one another by absorption spectroscopy. As expected, titration of

(+)-**1** with pyridine gave rather simple absorption and CD spectral changes, where the final spectra obtained were identical to those of (+)-**1** in the presence of a large excess (e.g., 3000 equiv) of *trans*-**2** (see Supporting Information, Figure S5). Nevertheless, for the objective of the present study, one of the most valuable results is the much higher affinity of *cis*-**2** than *trans*-**2** toward **1**, suggesting that the self-locking and unlocking of (+)-**1** are reversibly operative by photochemical isomerization of **2** (Scheme 1).

**Motion of (+)-1 upon Photoisomerization of 2.** Considering a rather poor ability of *trans*-**2** in photochemical isomerization,<sup>11</sup> along with the relative binding affinity of the isomeric forms of **2** toward **1**, we investigated a possibility of photoresponsive conformational change of (+)-**1** ( $4.2 \times 10^{-6}$  M) in the presence of 5.0 equiv of **2** with respect to (+)-**1**. In benzene at 20 °C, the mixture showed, in addition to an absorption band due to *trans*-**2** at 300 nm, characteristic visible absorption bands due to the zinc porphyrin units of (+)-**1**, which are virtually identical to those in the absence of *trans*-**2** (see Supporting Information, Figure S7). Upon irradiation at  $323 \pm 10$  nm to allow a *trans*-to-*cis* isomerization of **2**, the benzene solution displayed a monotonic decrease in intensity of the 300-nm absorption band.<sup>7</sup> At the same time, the Soret absorption band of (+)-**1** showed a blue shift from 433.0 to 428.0 nm with an isosbestic point at 430.0 nm (Figure 6a). This spectral change subsided in 90 min. As expected, the absorption spectral change thus observed was accompanied by a clear CD spectral change (Figure 6b), where the CD band due to (+)-**1** in the Soret absorption region was significantly enhanced and turned to show a split Cotton effect. Even more importantly, the CD band centered at 350 nm due to the ferrocene module of (+)-**1** exhibited an inversion of its sign from positive to negative, indicating a rotary motion of the ferrocene module. These spectral changes are quite analogous to those observed for (+)-**1** upon titration with *cis*-**2** (Figures 4b and S3). Therefore, the *cis* form of **2** is generated upon photoirradiation of *trans*-**2** and incorporated into (+)-**1** to form one-to-one complex (+)-**1**⊂*cis*-**2**. As observed by HPLC, 34 mol % of *trans*-**2** (1.7 equiv with respect to (+)-**1**) isomerized after the 90-min photoirradiation. Taking into account the association constant of *cis*-**2** toward (+)-**1**, the yield of (+)-**1**⊂*cis*-**2** was estimated as 93 mol %.

Upon exposure of the isomerized mixture to visible light ( $\lambda > 420$  nm) at 20 °C, an absorption spectral change opposite to the above took place to reach a plateau in 20 min (see Supporting Information, Figure S8). In particular, the appearance of the absorption band at 300 nm due to *trans*-**2** clearly indicates the occurrence of a backward *cis*-to-*trans* photoisomerization of **2**. Accordingly, the split Cotton effect at the Soret absorption band of the zinc porphyrin units disappeared with a reversal of the CD sense at 350 nm due to the ferrocene module (Figure 6c). HPLC analysis of the reaction mixture confirmed the presence of *trans*-**2** with only a trace amount of *cis*-**2** (<1 mol-%). As already described, this photochemical isomerization upon irradiation at  $\lambda > 420$  nm is most likely sensitized by the zinc porphyrin units in host **1** as a triplet photosensitizer.<sup>8</sup> In fact, *cis*-**2** itself did not isomerize upon direct photoexcitation but isomerized into its *trans* form in the presence of zinc tetraphenylporphyrin upon visible light irradiation. Hence, in our system,

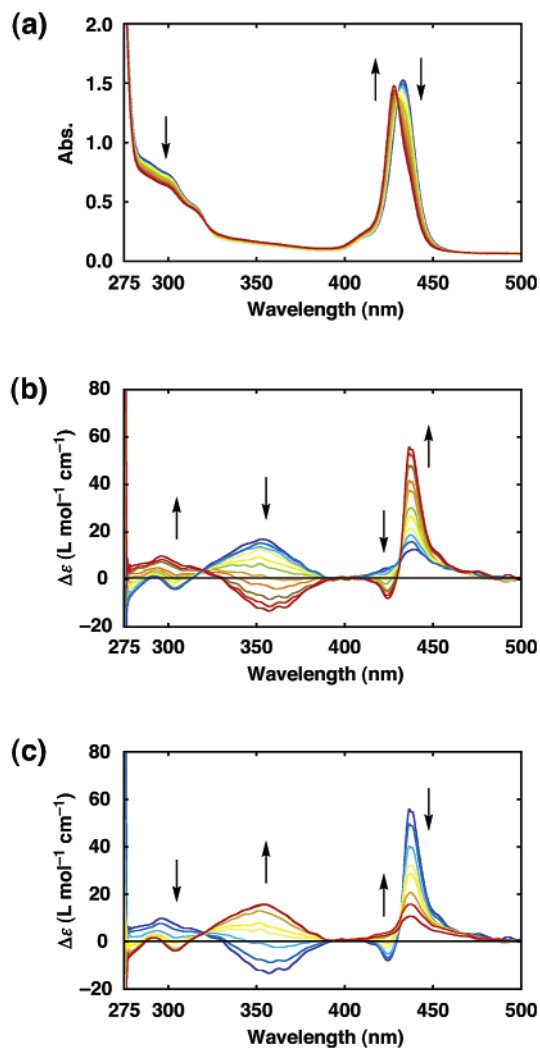
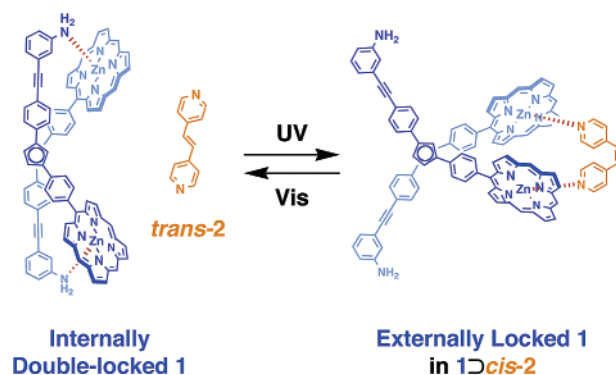


**Figure 6.** (a) Electronic absorption and (b) circular dichroism (CD) spectral changes of a mixture of (+)-**1** and *trans*-**2** ( $[(+)\text{-}1] = 4.2 \times 10^{-6}$  M;  $[trans\text{-}2]/[(+)\text{-}1] = 5.0$ ) in benzene at 20 °C upon irradiation with UV light ( $\lambda = 323 \pm 10$  nm) for 5.0, 10, 15, 20, 30, 40, 50, 60, 70, and 90 min. (c) CD spectral change of a mixture of (+)-**1** and **2** ( $[(+)\text{-}1] = 4.2 \times 10^{-6}$  M;  $[2]/[(+)\text{-}1] = 5.0$ ) in benzene at 20 °C upon irradiation with visible light ( $\lambda > 420$  nm) for 0.2, 0.5, 1.0, 2.0, 5.0, 10, and 20 min after 90-min UV irradiation in (b). Arrows indicate the directions of spectral changes.

a tight, two-point complexation between (+)-**1** and *cis*-**2** in the form of (+)-**1**⊂*cis*-**2** is considered to play an important role in the efficient photoisomerization of *cis*-**2**.

From all the above observations, it is obvious that, at  $[2]/[1] = 5.0$ , the internal lock of **1** cannot be unlocked by *trans*-**2**

(11) In the absence of **1** in benzene at 20 °C, irradiation of *trans*-**2** ( $3.4 \times 10^{-5}$  M) with UV light ( $\lambda = 323 \pm 10$  nm) resulted in a photostationary state in 7 h to furnish the ratio  $[cis\text{-}2]/[trans\text{-}2]$  of 87/13.

incapable of two-point complexation with **1**, but it is readily unlocked and fixed into an externally locked state (**1**  $\rightarrow$  *cis*-**2**) via a rotary motion, when *trans*-**2** is photoisomerized into *cis*-**2**. On the other hand, when *cis*-**2** in **1**  $\rightarrow$  *cis*-**2** is isomerized back into the *trans* form, the release of **2** from **1** takes place, thereby allowing **1** to spontaneously retrieve its internally locked state. Therefore, host **1** may be called a self-locking molecule, whose operation is switched on and off reversibly by using guest **2** as a photoresponsive key.

## Conclusions

By the combination with bispyridylethylene **2** as a photoreponsive key, we have demonstrated chiroptical visualization of the self-locking operation of a ferrocene-based chiral rotary host **1**. In this system, the intramolecular interaction (internal lock), operative between the zinc porphyrin and aniline units, is designed to compete with intermolecular interactions with photochromic **2**. Since the affinity of *cis*-**2** toward **1** is much higher than that of *trans*-**2**, the priority of these two competing interactions can be switched in response to the photochemical isomerization of **2**. Namely, the self-locking operation of **1** can be executed by the isomerization of *cis*-**2** in **1**  $\rightarrow$  *cis*-**2** into *trans*-**2**. When compared with the self-locking operation of a Ca<sup>2+</sup>/calmodulin-dependent kinase II system, where calmodulin serves as the key in response to Ca<sup>2+</sup> as the switching stimuli, our artificial system utilizes ultraviolet and visible light for enabling and disabling the unlocking function of **2** for self-locked **1**, respectively. While such a self-locking operation has not been focused yet in the design of artificial molecular machinery,<sup>3,4,9,12,13</sup> we believe that this conception may open a new door to stimuli-responsive molecular devices.

## Experimental Section

**Materials.** Toluene, Pd(PPh<sub>3</sub>)<sub>4</sub>, and Cs<sub>2</sub>CO<sub>3</sub> were purchased from Kanto Kagaku, Tokyo Chemical Industry, and Wako Chemicals, respectively, and used as received. *trans*-**2** was purchased from Aldrich and recrystallized from hexane. *cis*-**2** was synthesized according to the literature method.<sup>14</sup> For column chromatography, Wakogel C-300HG (particle size 40–60  $\mu$ m, silica) and Bio-Beads S-X3 (BIO RAD) were used.

**Measurements.** <sup>1</sup>H NMR spectra were recorded on JEOL type GSX-270 and GSX-500 spectrometers, where chemical shifts were determined with respect to nondeuterated or partially deuterated solvent

residues as internal standards. Matrix-assisted laser desorption/ionization time-of-flight mass (MALDI-TOF-MS) spectrometry was performed with a dithranol as a matrix on an Applied Biosystems BioSpectrometry Workstation model Voyager-DE STR spectrometer. Electronic absorption and infrared spectra were recorded on JASCO type U-best 560 and FT/IR-610 spectrometers, respectively. Circular dichroism (CD) spectra were recorded on a JASCO type J-720 spectropolarimeter.

**Methods.** Photoirradiation was carried out at 20 °C on degassed benzene solutions of samples in a 10-mm thick quartz cell under Ar, using a 150-W xenon arc lamp with a band-pass filter (Kenko) of  $\lambda = 323 \pm 10$  nm for UV irradiation or a cut filter (Kenko) of  $\lambda > 420$  nm for visible light irradiation. Titration experiments were conducted at 20 °C on benzene solutions of samples in a 10-mm thick quartz cell. Concentration dependencies of electronic absorption and CD spectra of benzene solutions of (+)-**1** were evaluated using 1, 10, and 50-mm thick quartz cells.

**Synthesis of (+)-**1**.**<sup>15</sup> Water (5 mL) was added to a toluene solution (20 mL) of a mixture of the zinc complex of 5-(4,4,5,5-tetramethyl-1,3,2-dioxaborolan-2-yl)-10,15,20-tri(4-methyl-phenyl)porphyrin<sup>16</sup> (157 mg,  $2.0 \times 10^{-4}$  mol), an enantiomer of **3**<sup>7</sup> (41 mg,  $4.6 \times 10^{-5}$  mol), Pd(PPh<sub>3</sub>)<sub>4</sub> (16 mg,  $1.4 \times 10^{-5}$  mol), and Cs<sub>2</sub>CO<sub>3</sub> (60 mg,  $1.8 \times 10^{-4}$  mol), and the resulting mixture was degassed by freeze–pump–thaw cycles and then refluxed under Ar for 10 h in the dark. Then, water (50 mL) was added to the reaction mixture, and the aqueous phase that separated was extracted with CH<sub>2</sub>Cl<sub>2</sub> ( $3 \times 100$  mL). The combined organic extract was dried over anhydrous Na<sub>2</sub>SO<sub>4</sub> and evaporated to dryness under reduced pressure. The powdery residue was chromatographed on Bio-Beads with toluene as an eluent, followed by silica gel with CH<sub>2</sub>Cl<sub>2</sub> as an eluent, to allow isolation of **1** as purple solid in 22% yield (20 mg,  $9.98 \times 10^{-6}$  mol). IR (KBr; cm<sup>-1</sup>): 3421, 2958, 2925, 2858, 1726, 1599, 1460, 1379, 1338, 1274, 1122, 1072, 997, 796, 719. <sup>1</sup>H NMR (270.05 MHz; CDCl<sub>3</sub>; 20 °C; ppm):  $\delta$  -2.36 (br, 4H), 1.24 (br, 2H), 2.48 (br, 2H), 2.66 (s, 12H), 2.71 (s, 6H), 5.01 (br, 2H), 5.12 (br, 2H), 5.53 (br, 2H), 5.87 (br, 2H), 6.14 (br, 2H), 7.40–7.50 (m, 16H), 7.54 (d, 8H,  $J = 7.7$  Hz), 7.92 (br, 8H), 8.03 (d, 4H,  $J = 7.7$  Hz), 8.11 (d, 4H,  $J = 7.3$  Hz), 8.77 (br, 4H), 8.81 (d, 4H,  $J = 4.5$  Hz), 8.88 (d, 4H,  $J = 4.5$  Hz), 8.98 (br, 4H). MALDI-TOF-MS (dithranol):  $m/z$  2005 ([M + H]<sup>+</sup> calcd: 2005). UV–vis (benzene):  $\lambda_{\text{max}}$  433.5, 563.0, 605.0 nm.

**Acknowledgment.** T.M. thanks the JSPS Young Scientist Fellowship. This research was partially supported by the Ministry of Education, Science, Sports and Culture, Grant-in-Aid for Scientific Research on Priority Areas “Life Surveyors” (to K.K.).

**Supporting Information Available:** Synthesis of 5-(4,4,5,5-tetramethyl-1,3,2-dioxaborolan-2-yl)-10,15,20-tri(4-methyl-phenyl)porphyrin and **4**. Absorption spectrum of **4**. Absorption spectra, titration data, and curve fitting profiles of (+)-**1** upon titration with *cis*-**2** and pyridine. This material is available free of charge via the Internet at <http://pubs.acs.org>.

JA0632308

(15) Miyaoura, N.; Suzuki, A. *Chem. Rev.* **1995**, *95*, 2457–2483.

(16) Murata, M.; Watanabe, S.; Masuda, Y. *J. Org. Chem.* **1997**, *62*, 6458–6459.

- (12) Selected reviews of molecular machinery: (a) Kinbara, K.; Aida, T. *Chem. Rev.* **2005**, *105*, 1377–1400. (b) Kelly, T. R. *Acc. Chem. Res.* **2001**, *34*, 514–522. (c) Collin, J.-P.; Dietrich-Buchecker, C.; Gaviña, P.; Jimenez-Molero, M. C.; Sauvage, J.-P. *Acc. Chem. Res.* **2001**, *34*, 477–487. (d) Balzani, V.; Credi, A.; Raymo, F. M.; Stoddart, J. F. *Angew. Chem., Int. Ed.* **2000**, *39*, 3348–3391.
- (13) Selected recent examples of molecular machines: (a) Fletcher, S. P.; Dumur, F.; Pollard, M. M.; Feringa, B. L. *Science* **2005**, *310*, 80–82. (b) Hernandez, J. V.; Kay, E. R.; Leigh, D. A. *Science* **2004**, *306*, 1532–1537. (c) Badjic, J. D.; Balzani, V.; Credi, A.; Silvi, S.; Stoddart, J. F. *Science* **2004**, *304*, 1308–1312. (d) Thordarson, P.; Bijsterveld, E. J. A.; Rowan, A. E.; Nolte, R. J. M. *Nature* **2003**, *424*, 915–918. (e) Ishii, D.; Kinbara, K.; Ishida, Y.; Ishii, N.; Okochi, M.; Yohda, M.; Aida, T. *Nature* **2003**, *423*, 628–632.
- (14) Whitten, D. G.; McCall, M. T. *Tetrahedron Lett.* **1968**, *9*, 2755–2758.